Evaluation results of the SmartLIM (Laser Interferometric Magnetometer) as a Traffic counter

Yukio Ikeda[*1] Koji Satori[*1] Shuichi Sunahara[*2] Hideo Ikegami[*3] Kazuhiro Kohga[*4]

Hitachi Cable, Ltd.[*1]
(5-1-1 Hidaka-cho, Hitachi, Ibaraki, JAPAN +81-294-25-3835, Ikeda.yukio@hitachi-cable.co.jp, Satori.koji@hitachi-cable.co.jp)
Toyota Motor Corporation[*2]
(7, Teihou, Teihou-cho, Toyota, Aichi, JAPAN +81-565-35-5747, shuichi_sunahara@mail.toyota.co.jp)
TechnoWave Inc.[*3]
(4-60, Shiga-cho, Kita-ku, Nagoya, Aichi, JAPAN +81-52-911-7552, HMikegami@aol.com)
Japan Electric Corporation[*4]
(7-7-6, Ueno, Taito-ku, Tokyo, JAPAN +81-3845-2611 kohga@jec-info.co.jp)

A fiber optical magnetometer, SmartLIM (Laser Interferometric Magnetometer), has been developed. The SmartLIM adopts the Mach-Zehnder interferometer to detect the local disturbance of the geomagnetic field produced by a car driven nearby. Its high sensitivity enables us to install the detector at a depth of 0.5m under the road surface, or beneath the underside of an elevated road. The SmartLIM was tested over four seasons under an elevated road following our factory site test. The results have confirmed its excellent detection capability and usefulness as a traffic counter.

Keywords: *Magnetometers, traffic counter, field test results*

1. Introduction

To ensure a smooth transportation conditions and safe traffic administration, various kinds of vehicle detectors are employed for traffic surveillance [1-4]. Currently the most widely used traffic detectors are ultrasonic and inductive loop detectors (USD and ILD respectively). These detectors have specific advantages and disadvantages as follows.

USD is easily installed and maintenance free, but poles or gantries are needed to mount the detector and they tend to be eyesores [2].

ILD obtains a high level of accuracy, but the sensor must be buried under the pavement. The installation and repair work involve digging and resurfacing the road, which are time consuming and cause traffic congestion [4]. Its application is also discouraged by its high failure rate [1], due to road distortion and repairing.

Compared to these sensors, the geomagnetic detectors have distinguishing features of easy installation and maintenance without generating any traffic disturbances or eyesores, once the detectors are installed deep under the road surface, or beneath the underside of an elevated road.

Until recently, research into geomagnetic detectors had been reported [5-9], but tended to show only temporal results or include an insufficiently accurate count compared to that obtained by currently used ultrasonic sensors in Japan, namely more than 97% [3].

To achieve high count accuracy and utilize the advantages of the geomagnetic detector under various road conditions, a high magnetic sensitivity and temperature stability are required.

We decided our target specifications based on the performance or test conditions of the ultrasonic sensors, such as a count accuracy exceeding 97% [3] and a temperature range of –20 to 60 ℃ [2].

To meet the requirements, we have developed a laser interferometric magnetometer (SmartLIM) with the use of the Mach-Zehnder interferometer technique, which has been well-known to detect minute physical quantities [10].

First, we fabricated a SmartLIM prototype and tested its performance as a magnetometer. Second, we performed a vehicle detection test by setting SmartLIM detectors under the road surface at our factory site. Then we installed the detectors on the underside of an elevated road and tested its capability as a traffic counter over four seasons. In these tests, SmartLIM showed satisfactory results.

2. Measurement principle of SmartLIM as a magnetometer

2.1 Specifications required for magnetometer

Because the bulk structure of a mechanized vehicle is comprised of a large mass of ferromagnetic materials, their presence is detectable by monitoring changes in the local geomagnetic field.

A car passing within around 0.3-1.0 m of a detector produces a local change in the geomagnetic field of around 7.5-30 μT [5-6]

In order to detect the vehicles by measuring changes in the magnetic field with high count accuracy, we tentatively decided on some specifications. The measurement range is $\pm 50\,\mu$T with the standard error (σ) of less than 0.25 μT, assuming that threshold level would be 0.75 μT, under the temperature range of –20 to 80℃.

2.2 Mach-Zhender interferometer [10]

Figure 1 shows the basic structure of a Mach-Zhender interferometer. The light source is launched into the fiber, then split into two beams of nominally equal intensity by an optical fiber coupler. Part is channeled through the sensing fiber while the remainder passes through the reference fiber. After traversing the sensing and reference fibers, these two fibers are recombined by the second optical fiber coupler. An interference signal between the two beams is then formed and subsequently detected by the photo detector.

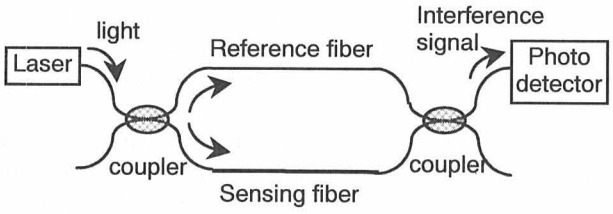

Figure 1. Structure of the Mach-Zhender Interferometer

2.3 Lorentz Force Fiber Optics

The Mach-Zhender interferometer detects the local change in sensing fiber. We apply this principle via Lorentz force.

As shown in the figure 2, both the sensing and reference fibers are coated with metal. When the metal of the sensing fiber carries current I[A] in the presence of magnetic field B[T], the sensor fiber will experience force F[N] given by [10];

$$F=I\times B \qquad (1)$$

Therefore the sensing fiber experienced a localize change in length. By combining those fibers and the mach-Zhender interferometer, known as Lorentz Force Fiber Optics(LFFO), the local geomagnetic field can be detected.

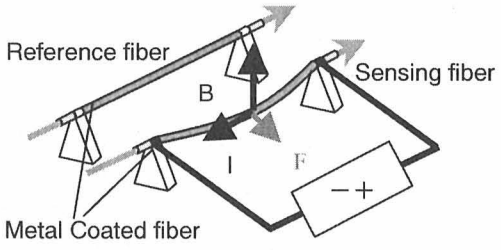

Figure 2. Lorentz force fiber Optics

Although the LFFO detects the geomagnetic field and local disturbance generated by a car, there are issues to consider based on the application as a traffic counter. They are the low resonance frequency [11] especially when detecting a high speed vehicle, and unstable output due to the tension instability caused by the configuration shown in figure 2.

To solve the conventional LFFO issues, we adopted a coiled metal coated fiber. The configuration is shown in figure 3.

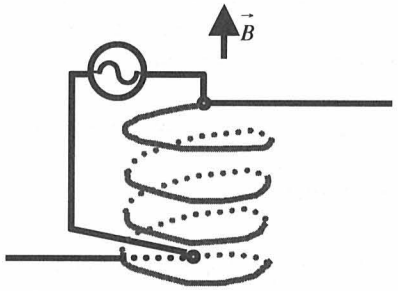

Figure 3. Configuration of coiled metal coated fiber

The bent portion of the metal coated fiber undergoes greater stress than the linear equivalent and represents substantially a rigid body by itself.

The equations of motion of the metal coated fiber coil are expressed by the formulae:

$$\rho A\ddot{\xi} - EI\xi^{(IV)} + T\xi'' = Bi\sin\omega t \qquad (2)$$

$$\rho A\ddot{\eta} - EI\eta'' = \kappa Bi\sin\omega t \qquad (3)$$

The representation of each character is as follows: ρ,mass density; A, a cross section of the fiber; E, Young modulus; I, fiber's moment of inertia; i, Alternating current; B, strength of magnet field perpendicular to the electric current i; ξ, minute displacement of the fiber in radius direction; η, a minute displacement of the fiber along a tangent to the fiber; κ,a constant which gives the contribution of Lorentz force to η supposing the contribution to ξ is 1. The dots and the primes over the characters express the time and space differentials,

respectively. (IV) refers to the fourth order space differential.

The equations provide the resonant frequencies, which traverse(ξ) vibration and longitudinal (η)vibration as follows:

$$\omega_t = \frac{n}{R\theta}\sqrt{\frac{aE}{R\rho}} \quad (4)$$

$$\omega_l = \frac{n}{R}\sqrt{\frac{E}{\rho}} \quad (5)$$

Here n is the mode number and R is the radius of the coil.

Judging by the comparison with the resonant frequencies calculated and measured, we conclude the main vibration mode to be longitudinal in nature as follows.

One of the examples is shown in figure 4. Here, conditions were; Au thickness , 3μm; Young modulus, E=7$\times 10^{10}$ N/m^2; mass density, ρ=3.86 $\times 10^3$ kg/m^3. The frequencies calculated using equation (5) and measured broadly correspond with each other while equation (4) provides around 1/40 of this value. Therefore, the resonance principle is based on longitudinal vibration and a high resonance frequency is obtained.

Since the resonance frequency depends on the radius of the coil, a smaller radius produces higher resonance frequency, provided the same optical fiber is used.

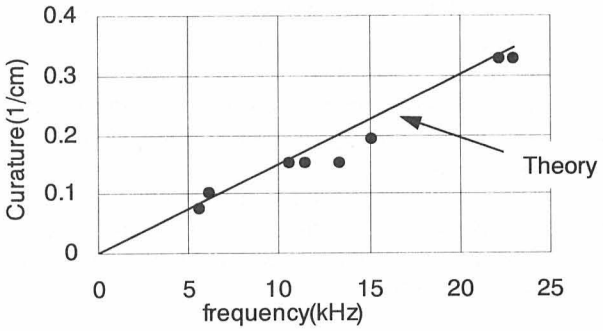

Figure 4. Relationship between resonance frequency and curvature[12]

In view of the estimated lifespan of the metal coated fiber, 58mm of the coil radius was determined. Figure 5 illustrates the metal coated fiber coil.

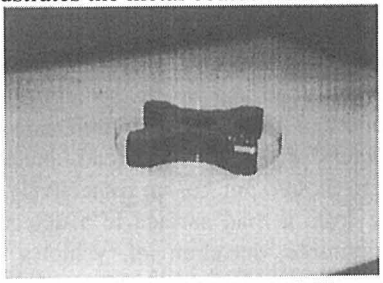

Figure 5. Metal coated fiber coil

2.4 SmartLIM basic structure

By using metal coated fiber coils, we fabricated the SmartLIM prototype, of which the basic structure is illustrated in Figure 6. The laser diode and photo detector are included in the signal processing unit. The detector is the Mach-Zehnder interferometer with metal coated fiber coils, converting the geometric field into strength of light. The sensing fiber coil carries RF currents to interact with the geomagnetic field via Lorentz force. The RF current frequency is adjusted to one of the resonant frequencies (20kHz in the present case) to optimize the detection capability. Phase shifters are used to stabilize the Mach-Zehnder interferometer under ambient temperature change. As for the optical fiber, two types of polarization maintaining fibers are used in order to reduce the bias drift. The phase shifters and the optical fibers were developed for fiber optic gyroscopes [13].

Since the change in the optical path-length within the interferometer is proportional to the vibrational amplitude along the coil, the interferometer output is detected as proportional to the degree of disturbance of the geomagnetic field produced by a vehicle passing above the sensing coil. .

The micro computer converts the analog signal to digital , which checks for the presence of a vehicle at 10 msec intervals. The computer also outputs the analogue voltage proportional to the magnetic field for parameter adjustment.

Figure 7 is a picture of the detector, used in the tests described in this paper.

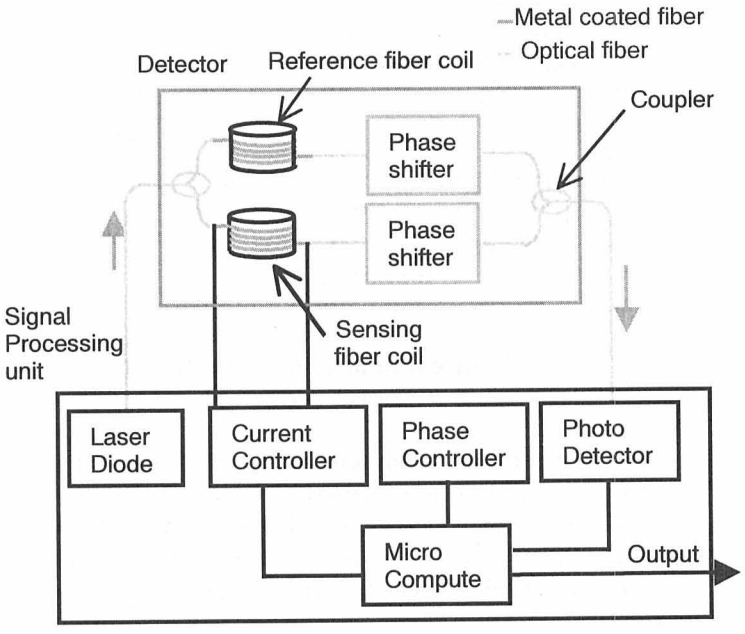

Figure 6. Basic structure of SmartLIM

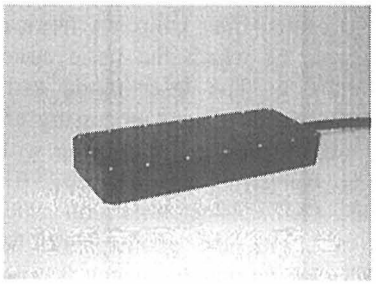

Figure 7. SmartLIM detector (40×350×140, 3kg)

3. Measurement Results

3.1. SmartLIM performance as Magnetometer

3.1.1 linearity. The detector was fixed in a 20 cm Helmholtz coil pair within a magnetic shield box. A -500 to 500 μT field was applied in the z axis.

The SmartLIM analogue output and its noise width are shown in figure 8.

Through regression analysis of this data, the standard error(σ) is 0.1 μT while the non linearity error is $\pm$ 0.2%

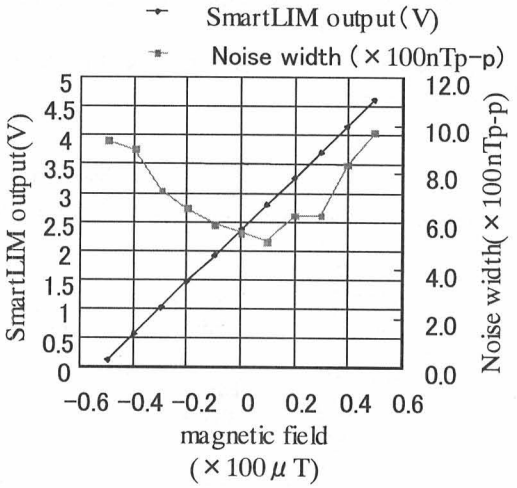

Figure 8 SmartLIM linearity and noise width

3.1.2.Temperature characteristics. The measuring equipment was set in a thermostatic chamber. Figure 9 shows the output fluctuation with a temperature range from –20 to 60 ℃, while 34 μ T, which is the geomagnetic field's strength in Tokyo, was applied to the detector.

The output fluctuated less than 2% over the temperature range when the temperature in the chamber was supposed to be stabilized.

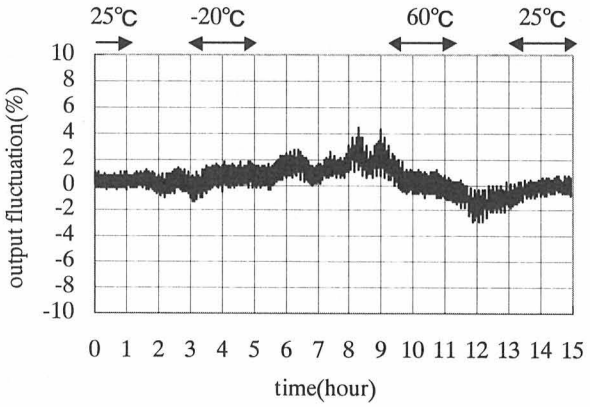

Figure9. Output fluctuation with temperature range of –20 to 60 ℃

3.2. Vehicle detection

SmartLIM was tested at our factory site for its vehicle detection ability. The detector was installed at a depth of 0.5 m under the road surface, then the SmartLIM analogue output was compared with that of the loop coil.

The cars tested were the Nissan AD van and Toyota Corolla, both of length 4.2m.

The analogue and loop coil outputs are shown in figure. 10, when the cars were driven above the detector. The horizontal dotted line, meanwhile, shows the geomagnetic level without any cars present.

The vertical dotted lines show the digital output range of SmartLIM, when threshold level is set at 0.2V. The only comparison may create certain pulses for one vehicle and pulses with short intervals are combined into one pulse when calculating with the micro computer for practical purposes.

The lengths of the car from the digital output are 4.0m and 3.5m respectively. The digital output is almost same as the loop coil output and SmartLIM has sufficient vehicle detection ability.

3.3. Traffic measurement

To evaluate the ability of SmartLIM for further practical use, the field tests were performed at highways of the Metropolitan Expressway (MEX). The count and speed accuracy were the primary parameters evaluated in the case of the traffic counter.

3.3.1. Count Test. First temporal volume test was performed at an elevated road and an intersection road. The detector was installed beneath the bottom side of each road. The thickness of the elevated road, and the intersection road were about 0.3m, 0.75m respectively.

The long distance from a road surface to a detector may result in undesirable detection of vehicles in adjacent lanes[9]. To eliminate the undesirable detection, we developed a signal processing method[14]. This

method utilizes the difference in geomagnetic disturbance caused by vehicles in adjacent lanes from those in the lane containing the detector.

By using SmartLIM and the signal processing method, a count accuracy of 99% was achieved at both sites [15], meaning the SmartLIM detection was successfully able to proceed, regardless of the road surface. Especially even at a distance of 0.75 m, a high accuracy was obtained and ferrous metal near the detector did not affect the performance.

Next, to check the long-time stability of the SmartLIM, we performed a thorough long term test throughout four seasons at the elevated road location. As shown in figure 11, a detector was also installed on the underside of the road using an aluminum support to avoid any damage to the road.

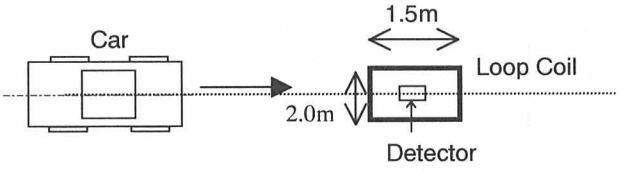

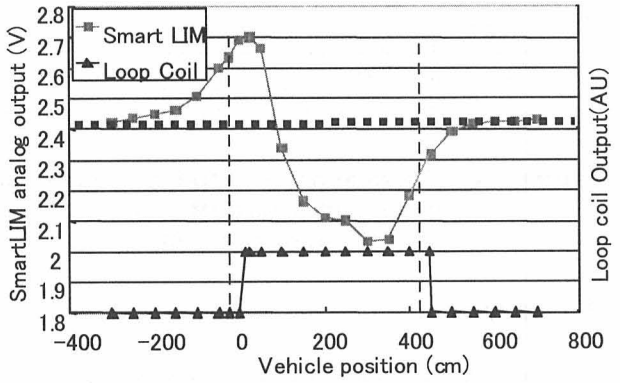

(a) Nissan AD van

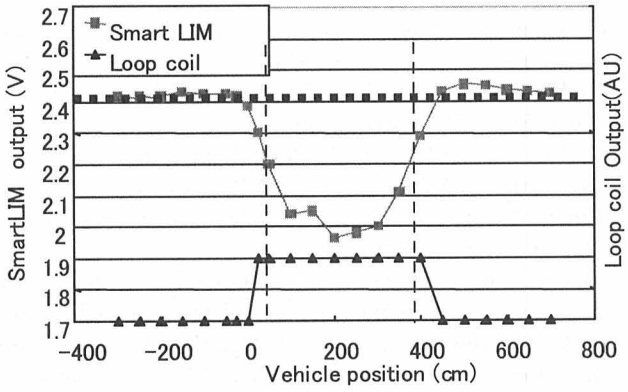

(b) Toyota Corolla

Figure 10 SmartLIM analogue output and Loop coil output

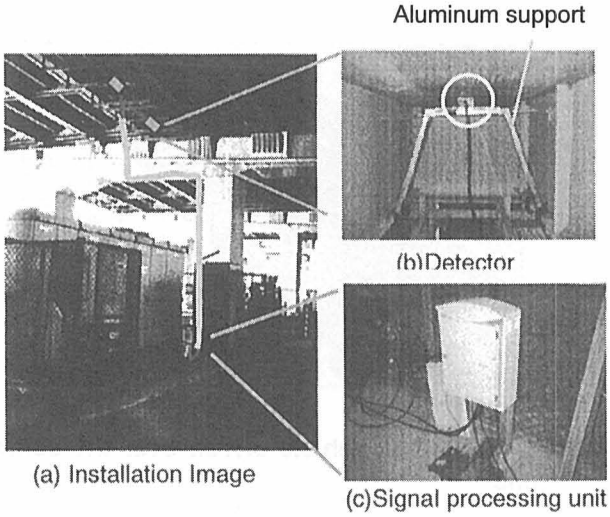

Figure 11 SmartLIM Installation for long term test

The test results are shown in Table 1. Each test period was 20 minutes. The SmartLIM achieved its target specification of over 97% and its performance was not degraded by temperature and long term placement.

Table 1 Count Accuracy

Date	Temp	Visual observation	SmartLIM Output	Accuracy
'02/11/7	11℃	210	212	99%
'03/2/14	11℃	227	229	99%
'03/5/28	24℃	189	191	99%
'03/8/27	26℃	120	119	99%

As an example, one minute of count data from the visual observation and the SmartLIM output of December 7th in 2002 are shown in figure. 12.

At times of 3 and 12 minutes respectively, the SmartLIM unit overcounted. This was caused by vehicles driven over the center line and an example is shown in figure 13.

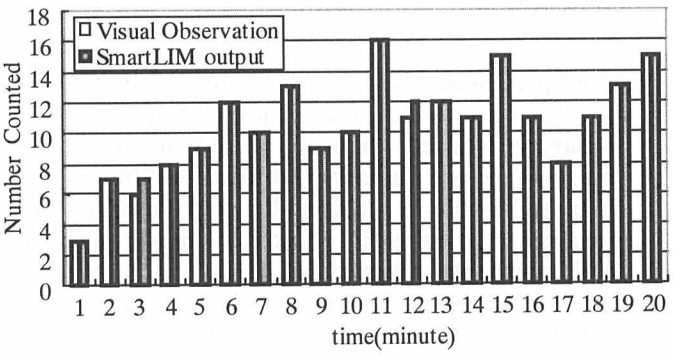

Figure 12. SmartLIM count accuracy for December 11, 2002

Figure 13 Vehicle driven over the center line

To investigate the effect of different vehicle types, the data of December 7th in 2002, except for the overcounted portion, is itemized in Table 2.

Automobiles and trucks were counted with a degree of high accuracy while motor cycles were not counted since they exerted a smaller geomagnetic disturbance than the threshold level.

Current traffic counters also need not include accurate counts of motor cycles, meaning SmartLIM displayed excellent performance as a practical traffic counter.

Table 2 Count accuracy for Vehicle's types for December 11, 2002

Type	Visual observation	SmartLIM output
Auto	71	71
Container Truck	51	51
Truck	35	35
Station Wagon	20	20
Oil tanker truck	8	8
Light duty truck	8	8
Trailer	6	6
Crane truck	5	5
Recreational Vehicle	3	3
Bus	2	2
Motor cycle	2	0

3.2.2 Speed test. Using two detectors installed in the same lane, the speed of a vehicle driven above the detectors is obtained. The speed is calculated using the spacing of the two detectors and the time difference of the pulse rise times recorded by each detector. The spacing of the test was 5m, which is a standard value for the ultrasonic sensors used in MEX[3].

The speed accuracy was evaluated based upon a repetitive review of videotapes for 10 minutes each.

As representative traffic conditions to save evaluation time and cost, free-flow and stop-and-go conditions were selected, considered to give the highest and lowest speeds of usual traffic flow respectively.

Figure 14 shows the speed correlation between the video and SmartLIM data. The solid line is provided as a visual aid for the reader. The data shown as circles were one minute averages calculated using the formula:

$$e = \frac{1}{n}\sum_{i=1}^{n}\left|P_i - A_i\right| \quad (6)$$

Here Pi is the value measured with SmartLIM and Ai is the value measured using the Video data.

The error during free-flow and stop-and-go traffic conditions were 6.0 km/h and 1.8 km/h, respectively. These values were good enough to be used in current traffic surveillance applications.

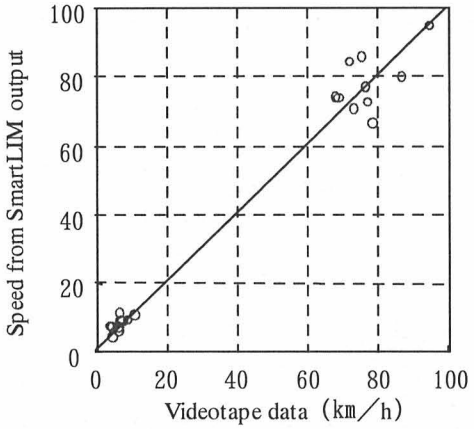

Figure 14. Correlation of speed based on video and SmartLIM data for August 27, 2003

4. Conclusion

To achieve the advantage of geomagnetic detection for a traffic counter under various road conditions, a new fiber optical magnetometer, SmartLIM, has been developed with the use of the Mach-Zehnder interferometer technique.

A SmartLIM prototype was fabricated and its basic performance as a magnetometer evaluated. It displays high sensitivity and low fluctuation with a temperature range from –20 to 60 degrees.

We then performed the long term test to verify the long-term stability of SmartLIM. In the tests, the SmartLIM detectors were mounted beneath the bottom side of the elevated road

The longtime test results showed that SmartLIM achieved a high count accuracy of 99% in each season and its performance was not degraded by temperature and long time placement. SmartLIM also displays accurate speed detection ensuring its role as a sensor for the traffic surveillance.

Throughout the test, the sensor units are easily installed and were very reliable during the test periods.

As a traffic counter, SmartLIM provided accurate speed and volume results at the test site.

In terms of commercialization, the cost, interface to host system and the detector installment still have to be clarified. Although SmartLIM is still in an R&D stage, we estimate that the cost will be equivalent to current traffic counters. As for the interface and system installment, we are planning to conduct certain trials in fields adjusting them for specific customers. The results will be reported.

5. Acknowledgement

The authors wish to thank the Metropolitan Expressway Public Corporation for making the field tests performed in this study available.

6. References

[1]N. H. C. Yung, K. C. Chan and A. H. S. Lai, "Vehicle-Type Identification through Automated Virtual Loop assignment and Block-Based Motion Estimation", Proceedings of IEEE conference on Intelligent Transportation Systems, Tokyo, October 1999,pp.692-702

[2]N. Ushio, "Loop vs Ultrasonic In Chicago: Ultrasonic Vehicle Detector Field Test Isolating Diffused Reflection and Enduring Harsh Environment", Proceeding of 5th world congress on Intelligent Transportation systems, Soul October 1998

[3]T. Matsuo, Y. Kaneko, M. Matano, "Introduction of Intelligent vehicle detection sensors", Proceedings of IEEE conference on Intelligent Transportation Systems, Tokyo, October 1999

[4]S.W. Kim et al, "Performance Comparison of Loop/piezo and Ultrasonic Sensor-based Traffic Detection Systems for Collecting Individual Vehicle Information", proceedings of 5th world congress on Intelligent Transportation systems, October 1998

[5] Takeshi Kawai, "Application of magnetic sensor for vehicle detection", Proceedings of 9th Transportation and Logistics Conference, Japan Society of Mechanical Engineers, Kawasaki(Japan),December 2000, pp.265-266(in Japanese)

[6]M. J. Caruso, "Vehicle Detection and Compass Applications using AMR Magnetic Sensors", Proceedings of Sensors Exp., Baltimore, 1999, pp477-489

[7]Takashi Arai and Hisao Ono, "An observation of magnetic patterns of a moving object by flux-gate magnetometer," T.IEE Japan, Vol.121-E, NO.1, 2001, pp.8-13(in Japanese)

[8] T. Oda et al, "Verification of Precision of Traffic Count and the Proposal of Best Using Traffic Count", Proceedings of Cold region Technology Conference '98, Japan, December 1998, pp87-91(in Japanese)

[9] Dan Middleton and Rick Parker, "Initial Evaluation of Selected Detectors to Replace Inductive Loops on Free ways", PB report, PB-2001-103539, April 2000

[10]Eric Udd, Fiber Optic sensors: An introduction for Engineers and scientists, John Wiley & Sons, New York, 1991

[11]H. Okamura, "Fiber-Optic magnetic sensor utilizing the Lorentzian force", J. light wave Technology., Vol. 8,1990, pp1558-1564

[12]Koji Satori, Yukio Ikeda and Hideo Ikegami, "Study on Optical Fiber Magnetometer Using Mach-Zhender Interferometer", Technical report of the Institute of Electronics, Information and Communication Engineers(IEICE), OFT2003-6, June, 2003, pp21-24

[13]Yukio Ikeda, Toshiya Yuhara, Tatsuya Kumagai, Hirokazu Soekawa and Hiroshi Kajioka, "Development of Fiber Optic Gyroscopes for Industrial and Consumer Applications", Proceedings of The international Society for Optical Engineering(SPIE), Volume 2394, November, 1994, pp73-86

[14]Yukio Ikeda, Shuichi Sunahara, patent pending, 2002-201243.

[15]Yukio Ikeda, Shuichi Sunahara, Hideo Ikegami and Kazuhiro Kohga, "Development of Fiber Optical Magnetometer, SmartLIM(Laser Interferometric Magnetometer), for Traffic counter", proceedings of the 9th world congress on Intelligent Transportation systems, Chicago, October 2002

Yukio Ikeda received B.E. and M.E. degrees in electrical and electronic engineering from the Toyohashi University of Technology in 1987 and 1989 respectively. He works at the Advanced Technology Laboratory, Hitachi Cable, Ltd, as the sensor system group manager. His research interests include fiber optic sensor systems. He is a member of the Institute of Electronics, Information and Communication Engineers (IEICE) of Japan.

Kouji Satori received a B.E. degree in physics from Tokyo University of Science in 1989 and an M.E. degree in physics from the Tokyo Institute of Technology in 1991. He works at the Advanced Technology Laboratory, Hitachi Cable , Ltd. as a researcher. His research interest is fiber optic sensors.

Shuichi Sunahara works for Toyota Motor Corporation. His main work involves the Development of ERP, ETC and sensor systems.

Hideo Ikegami is the president of Technowave Inc., honorary professor of Nagoya University and the National Institute of Fusion Science. His research interest is plasma physics and nuclear fusion.

Kazuhiro Kohga works for Japan Electric Corporation. after previously working for the Metropolitan Public Expressway corporation. His current post is consultant in the field of ITS.

Received: 8 May 2004
Revised: 23 August 2004
Accepted: 3 September 2004
Editor: Sadayuki Tsugawa